



# Treball Final de Grau

**Preparation of a mixed-valence Co(III)-Fe(II) cubic complex and kinetic study of its redox reactivity with peroxodisulfate.**

**Preparació d'un compost cúbic de valència-mixta Co(III)-Fe(II) i estudi cinètic de la seva reactivitat redox amb peroxodisulfat.**

Aina Qeral Beltran

*June 2019*



UNIVERSITAT DE  
BARCELONA

**B:KC** Barcelona  
Knowledge  
Campus  
Campus d'Excel·lència Internacional



Aquesta obra està subjecta a la llicència de:  
Reconeixement–NoComercial–SenseObraDerivada



<http://creativecommons.org/licenses/by-nc-nd/3.0/es/>



*Hem d'estar disposats a renunciar a la vida que hem planejat per poder gaudir de la vida que ens està esperant.*

Joseph Campbell

Per començar, m'agradaria agrair al Dr. Manel Martínez, primer de tot per tota la paciència que ha (ens hem) tingut durant aquests mesos, però sobretot perquè ha estat un molt bon tutor del qui he après molt. També donar-li les gràcies a la Dra. Montserrat Ferrer i tant al Miguel com a l'Albert per tota l'ajuda que m'han donat, un al començament i l'altre al final del treball.

Finalment agrair a la família i als amics per aguantar-me en tots els moments de nervis i estrès viscuts durant aquests anys, sobretot durant aquests últims mesos. Moltes gràcies per tot el suport rebut per part de tots en els moments més difícils, he pogut arribar fins aquí gràcies a vosaltres.



# REPORT



# CONTENTS

|  |    |
|--|----|
| <b>1. SUMMARY</b>  | 3  |
| <b>2. RESUM</b>  | 5  |
| <b>3. INTRODUCTION</b>   | 7  |
| <b>4. OBJECTIVES</b>   | 11 |
| <b>5. EXPERIMENTAL</b>   | 13 |
| 5.1. Materials and methods   | 13 |
| 5.2. Synthesis of $[\{Co^{III}(Me_3TACN)_4\}\{\mu-Nc\}_3\{Fe^{II}(CN)_6\}_4]^{4-}$ (Cube)            | 13 |
| 5.2.1. Synthesis of $[Co^{III}(Me_3TACN)(NO_2)_3]$   | 13 |
| 5.2.2. Synthesis of $[Co^{III}(Me_3TACN)Cl_3]$   | 13 |
| 5.2.3. Synthesis of $Na_4[\{Co^{III}(Me_3TACN)_4\}\{\mu-Nc\}_3\{Fe^{II}(CN)_6\}_4]$ (Na-Cube)        | 14 |
| 5.2.4. Synthesis of $K_4[\{Co^{III}(Me_3TACN)_4\}\{\mu-Nc\}_3\{Fe^{II}(CN)_6\}_4]$ (K-Cube)          | 15 |
| 5.3. Preparation of Fully oxidized Cube $[\{Co^{III}(Me_3TACN)_4\}\{\mu-Nc\}_3\{Fe^{III}(CN)_6\}_4]$ | 15 |
| 5.4. Kinetics of the oxidation of Cube   | 16 |
| 5.4.1. Preparation of Buffers  | 16 |
| 5.4.2. Preparation of stock solutions of the reactants   | 17 |
| 5.4.3. Oxidation reaction  | 17 |
| <b>6. RESULTS AND DISCUSSION</b>   | 19 |
| 6.1. Synthesis of Cube   | 19 |
| 6.2. Preparation of oxidized Cube  | 19 |
| 6.3. Modelling the time-resolved spectral changes  | 20 |
| 6.4. Study and interpretation of the effect of pH and concentration of $[S_2O_8]^{2-}$               | 23 |
| 6.5. Redox mechanism   | 25 |
| 6.5.1. Oxidation reaction  | 25 |
| 6.5.2. Reduction reaction  | 26 |
| <b>7. CONCLUSIONS</b>  | 27 |
| <b>8. REFERENCES AND NOTES</b>   | 29 |

|                          |    |
|--------------------------|----|
| <b>APPENDICES</b>        | 31 |
| Appendix 1: Kinetic data | 33 |

# 1. SUMMARY

The oxidation of Fe<sup>II</sup> in the newly prepared and characterised mixed-valence complex  $[\{Co^{III}(Me_3TACN)_4\}\{\mu\text{-NC}\}_3\{Fe^{II}(CN)_6\}_4]^{4-}$  has been studied as a function of pH and the concentration of the oxidizing agent. The oxidation reaction has been carried out with peroxodisulfate and consists of a fourth-step process with the participation of solvent-assisted outer-sphere complexes, as a result of the establishment of hydrogen bonds that involve the oxo groups of the oxidant (peroxodisulfate), the water molecule of the reaction medium and the terminal cyanido ligands of the octametallate cube. The reduction reaction, by hydroxide ions, of the fully oxidized  $[\{Co^{III}(Me_3TACN)_4\}\{\mu\text{-NC}\}_3\{Fe^{III}(CN)_6\}_4]$ , takes place producing hydrogen peroxide from water even at neutral or slightly acidic pH. The kinetic parameters for the oxidation reaction have been determined and are indicative of above mentioned outer-sphere precursor formation. While for the oxidation of the initial mixed-valence  $\{Co^{III}/Fe^{II}\}_4^{4-}$  and partially oxidized  $\{Co^{III}_4/Fe^{II}_3Fe^{III}\}^{3-}$  complexes, the outer-sphere precursor formation equilibrium constants,  $K_{OS}$ , are large enough for the observation of limiting kinetics in their oxidation reaction rate-determining steps, for the oxidation of the intermediate  $\{Co^{III}_4/Fe^{II}_2Fe^{III}_2\}^{2-}$  and  $\{Co^{III}_4/Fe^{II}Fe^{III}_3\}^-$  complexes the buildup of outer-sphere precursor complexes with peroxodisulfate has not been detected.

**Keywords:** Cobalt / Iron / Mixed-valence complexes / Redox processes.



## 2. RESUM

L'oxidació per un mecanisme d'esfera externa de Fe<sup>II</sup> al nou complex de valència mixta preparat i caracteritzat  $[(\text{Co}^{\text{III}}(\text{Me}_3\text{TACN}))_4\{\mu\text{-NC}\}_3\{\text{Fe}^{\text{II}}(\text{CN})_6\}_4]^{4-}$  ha estat estudiada com a funció del pH i de la concentració de l'agent oxidant. La reacció d'oxidació s'ha dut a terme amb peroxodisulfat i consisteix en un procés de quatre etapes amb la participació de complexos d'esfera externa assistits per el dissolvent, com a resultat de l'establiment de enllaços d'hidrogen que impliquen els grups oxo de l'oxidant (peroxodisulfat), les molècules d'aigua del medi de reacció i els lligands terminals del cianur del cub octametàl·lic. La reacció de reducció, mitjançant ions hidròxid, del complex totalment oxidat  $[(\text{Co}^{\text{III}}(\text{Me}_3\text{TACN}))_4\{\mu\text{-NC}\}_3\{\text{Fe}^{\text{III}}(\text{CN})_6\}_4]$ , té lloc produint peròxid d'hidrogen a partir de l'aigua fins i tot a pH neutre o lleugerament àcid. S'han determinat els paràmetres cinètics per a la reacció d'oxidació i són indicatius de la formació dels precursors d'esfera externa mencionats anteriorment. Mentre que per als complexos de valència-mixta inicial  $\{\text{Co}^{\text{III}}/\text{Fe}^{\text{II}}\}_4^{4-}$  i parcialment oxidat  $\{\text{Co}^{\text{III}}_4/\text{Fe}^{\text{III}}_3\text{Fe}^{\text{II}}\}_3^{3-}$ , les constants d'equilibri de formació del precursor d'esfera externa,  $K_{\text{OS}}$ , són prou grans com per observar la cinètica limitant en les seves etapes determinants de la velocitat de la reacció d'oxidació, en els complexos intermedis  $\{\text{Co}^{\text{III}}_4/\text{Fe}^{\text{II}}_2\text{Fe}^{\text{III}}_2\}_2^{2-}$  i  $\{\text{Co}^{\text{III}}_4/\text{Fe}^{\text{II}}\text{Fe}^{\text{III}}_3\}$  la formació de complexos precursors d'esfera externa amb peroxodisulfat no s'ha detectat.

**Paraules clau:** Cobalt / Ferro / Complexos de valència mixta / Processos redox.



### 3. INTRODUCTION

For some years now, the formation of cyanido-bridged mixed-valence complexes and their redox reactivity has been studied.<sup>[1–13]</sup> There is an increasing interest in these complexes, at least in part, due to their particular structural, charge transfer, redox, and spectroscopic properties.<sup>[11]</sup>

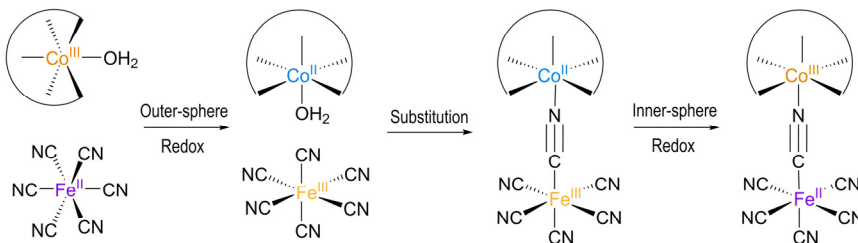
Mixed-valence complexes, particularly those that involve cyanido-bridged structures, have been studied mainly due to their great interest because of their properties derived from the presence of a metal-to-metal charge-transfer electronic transition (MMCT).<sup>[1,14,15]</sup> These properties are of relevance to magnetic,<sup>[10]</sup> optical and catalytic activity, and use as possible electrochromic materials.<sup>[16]</sup> Possible applications of electrochromic materials include “smart windows” or displays, which are able to modulate light transmittance electronically, solar energy conversion, data storage and sensors.<sup>[7]</sup> For this reason, they continue to attract considerable attention.

These mixed-valence complexes have an important characteristic, all of them have been observed to have intense colours arise from these MMCT transitions, where an electron is transferred, for example, from a Fe<sup>II</sup> to a Co<sup>III</sup> centre. The MMCT transition would not be possible in the oxidized (Co<sup>III</sup>-Fe<sup>III</sup>) or reduced (Co<sup>II</sup>-Fe<sup>II</sup>) states, resulting in loss of this intense colouration. Thus, they have potential use on electrochromic materials.

In order to provide a better understanding of the electronic properties of these species, the redox processes that involve the disappearance and appearance of these charge-transfer bands, in the UV-Vis or near-IR zone of the electromagnetic spectrum, have been studied for a lot of metal and ligands combinations.<sup>[16]</sup>

Several outer-sphere redox reactions of macrocyclic complexes of Co<sup>III</sup> with [Fe(CN)<sub>6</sub>]<sup>4-</sup> have been studied. There, the importance of the reorganization of the solvent in the process has been shown to be crucial for differences in the derived thermal activation parameters. In addition, the existence of a strong outer-sphere complexation, before the rate-determining of electron-transfer, has been found to be a dominant factor.<sup>[4,9,17,18]</sup>

From these studies, the formation of discrete mixed-valence complexes of  $\text{Co}^{\text{III}}/\text{Fe}^{\text{II}}$ , produced by an inner-sphere redox process from the reduced macrocyclic complexes of  $\text{Co}^{\text{II}}$  and the corresponding ligand  $[\text{Fe}(\text{CN})_6]^{3-}$  has been proposed (Scheme 1). More studies on these compounds have led to the complete characterization of a series of  $\text{Fe}^{\text{II}}\text{CNC}\text{Co}^{\text{III}}$  mixed-valence complexes with different macrocycles and geometries around the  $\text{Co}^{\text{III}}$  centre.<sup>[6–8]</sup>



Scheme 1: General mechanism of the formation of cyanido-bridged mixed-valence of  $\text{Co}^{\text{III}}$  and  $\text{Fe}^{\text{II}}$ .<sup>[11]</sup>

Self-assembly of macrocyclic metal complexes is a powerful method for the construction of well-defined architectures. In the last years, different dimers of  $\text{Fe}(\text{II})$  with cyanido ligands and  $\text{Co}(\text{III})$  with pentaamine macrocyclic ligands have been prepared and studied (Figure 1). Then, in order to increase the nuclearity, tri- and tetranuclear complexes have been synthesized and their redox processes have been studied.<sup>[3,4,9,11–13,17,18]</sup>

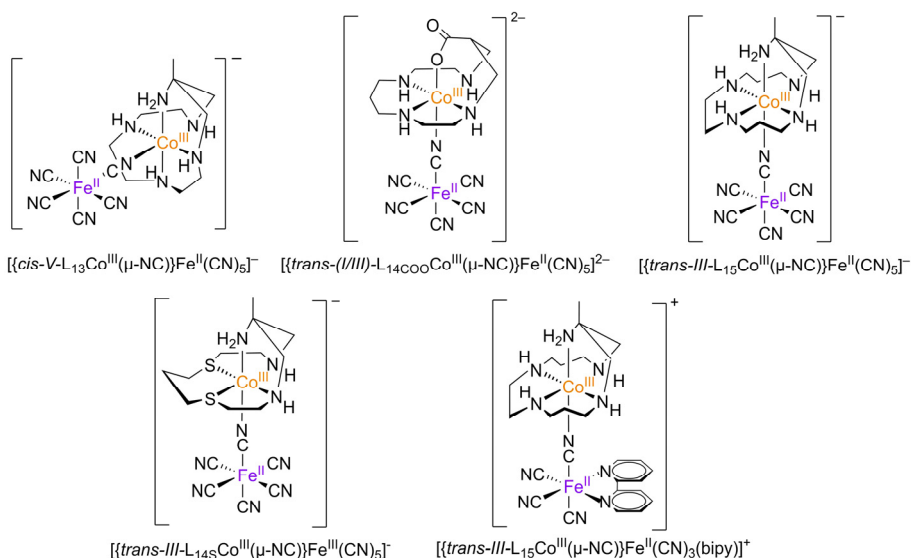


Figure 1: Examples of cyanido-bridged mixed-valence dimers previously prepared.<sup>[13]</sup>

Recently, the preparation of a diamagnetic cyanido-bridged  $[\{Co^{III}\{(Me)_2(\mu-ET)cyclen\}\}_2\{(\mu-NC)_2Fe^{II}(CN)_4\}_2]^{2-}$  square complex<sup>[4,18]</sup> (Figure 2) via the above-mentioned mechanistically designed, self-assembly reaction has been reported. This process involves the expected rate-limiting outer-sphere redox reaction, followed by a fast substitution/inner-sphere redox reaction similar to that indicated in Scheme 1.

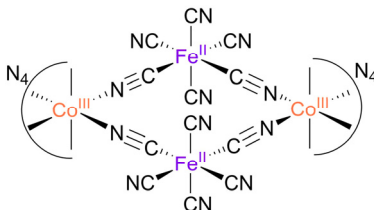


Figure 2: Cyanido-bridged Square complex  $[\{Co^{III}\{(Me)_2(\mu-ET)cyclen\}\}_2\{(\mu-NC)_2Fe^{II}(CN)_4\}_2]^{2-}$ .

This fact opens up the possibility of synthesizing higher nuclearity cyanido-bridged mixed-valence complexes  $\{Co^{III}/Fe^{II}\}_4$  with “cubic” shape<sup>[5]</sup> by the correct choice of the encapsulating ligand attached to the cobalt centre. For example  $[\{Co^{III}(Me_3TACN)\}_4\{(\mu-NC)_3Fe^{II}(CN)_6\}_4]^{4-}$  that is illustrated in Figure 3.

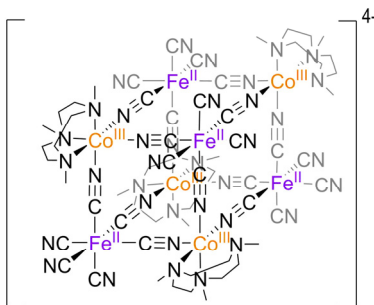


Figure 3:  $[\{Co^{III}(Me_3TACN)\}_4\{(\mu-NC)_3Fe^{II}(CN)_6\}_4]^{4-}$  (Cube)



## 4. OBJECTIVES

The aim of this work is to prepare a cyanido-bridged mixed-valence complex with cubic shape  $[\{Co^{III}(Me_3TACN)\}_4\{\mu-NC\}_3\{Fe^{II}(CN)_6\}_4]^{4-}$  (Cube).

Characterise these compounds by: Nuclear Magnetic Resonance  $^1H$ -NMR and  $^{13}C$ -NMR, Ultraviolet-Visible spectroscopy (UV-Vis), Infrared spectroscopy (IR), Mass spectroscopy (MS) and Inductively Coupled Plasma (ICP). Make a comparison of the product obtained if sodium or potassium salts are used as a reactive.

Prepare and characterise the fully oxidized Cube  $[\{Co^{III}(Me_3TACN)\}_4\{\mu-NC\}_3\{Fe^{III}(CN)_6\}_4]$ .

Carry out a series of kinetic studies for the oxidation reaction of the  $[\{Co^{III}(Me_3TACN)\}_4\{\mu-NC\}_3\{Fe^{II}(CN)_6\}_4]^{4-}$  complexes with peroxodisulfate and study the effect of pH in this reaction.

Determine the chemical behaviour of reactions by UV-Vis spectroscopy, analyse the dependence of the pseudo-first-order reaction rate constants with the concentration of peroxodisulfate to determine the rate constant of the reaction steps, and interpret the kinetic parameters obtained in order to understand the reaction mechanism.



## 5. EXPERIMENTAL

### 5.1. MATERIALS AND METHODS

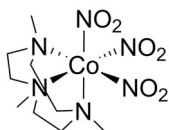
$\text{Na}_4[\text{Fe}(\text{CN})_6]$  was recrystallized following the procedure previously established in the laboratory. All other reactants were obtained commercially from different companies and were used without further purification.

### 5.2. SYNTHESIS OF $[\{\text{Co}^{\text{III}}(\text{Me}_3\text{TACN})\}_4\{\mu\text{-NC}\}_3\{\text{Fe}^{\text{II}}(\text{CN})_6\}_4]^{4-}$ (CUBE)

#### 5.2.1. Synthesis of $[\text{Co}^{\text{III}}(\text{Me}_3\text{TACN})(\text{NO}_2)_3]$

$[\text{Co}^{\text{III}}(\text{Me}_3\text{TACN})(\text{NO}_2)_3]^{19}$  was obtained from the reaction of 2.9 g (42 mmol) of  $\text{NaNO}_2$  and 3.6 g (12 mmol) of  $\text{Co}(\text{NO}_3)_2 \cdot 6\text{H}_2\text{O}$  in 20  $\text{cm}^3$  of a 1.0 M aqueous solution of acetic acid and sodium acetate. Then, a solution of 1.5 g (9 mmol) of  $\text{Me}_3\text{TACN}^{19,20}$  (1,4,7-Trimethyl-1,4,7-triazacyclononane, stabilized in  $\text{NaHCO}_3$ ) in 16  $\text{cm}^3$  of water was added slowly and fumes of  $\text{NO}_2$  were observed. The solution was stirred for two hours and, after this time, a dark brown solid had precipitated. It was washed with 10-20  $\text{cm}^3$  of water, ethanol and acetone and was taken to dryness.

1.5 g of  $[\text{Co}^{\text{III}}(\text{Me}_3\text{TACN})(\text{NO}_2)_3]$  of a mixture of nitro ( $\text{NO}_2$ ) and nitrite ( $\text{ONO}$ ) were obtained with a yield of 46%.



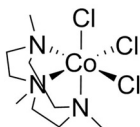
Brown solid. IR<sup>[21-23]</sup> (KBr): 1429, 1382, 1306 ( $\text{NO}_2$ ), 822 ( $\text{ONO}$ )  $\text{cm}^{-1}$ .

#### 5.2.2. Synthesis of $[\text{Co}^{\text{III}}(\text{Me}_3\text{TACN})\text{Cl}_3]$

$[\text{Co}^{\text{III}}(\text{Me}_3\text{TACN})\text{Cl}_3]^{19}$  was obtained from the reaction of 1.5 g (4.1 mmol) of  $[\text{Co}^{\text{III}}(\text{Me}_3\text{TACN})(\text{NO}_2)_3]$  (previously prepared) in 50  $\text{cm}^3$  of  $\text{HCl}$  1.0 M (dark orange solution)

after heating at 80 °C for about an hour. During the reaction, orange fumes (NO<sub>2</sub>) evolved and the solution became dark blue. The final solution was taken to dryness in a rotary evaporator and a dark blue/green solid was obtained. This solid was washed several times with 10-20 cm<sup>3</sup> of ethanol and acetone and left to air-dry. The mother liquor had a turquoise colour and the product was a dark blue solid.

1 g of [Co<sup>III</sup>(Me<sub>3</sub>TACN)Cl<sub>3</sub>] were obtained with a yield of 74%.



Dark blue solid. IR<sup>[21-23]</sup> (KBr): 2998, 2934 (-C-H), 1573, 1542, 1500 (C-N) cm<sup>-1</sup>.

### 5.2.3. Synthesis of Na<sub>4</sub>[(Co<sup>III</sup>(Me<sub>3</sub>TACN))<sub>4</sub>{(μ-NC)<sub>3</sub>Fe<sup>II</sup>(CN)<sub>6</sub>}]<sub>4</sub> (Na-Cube)

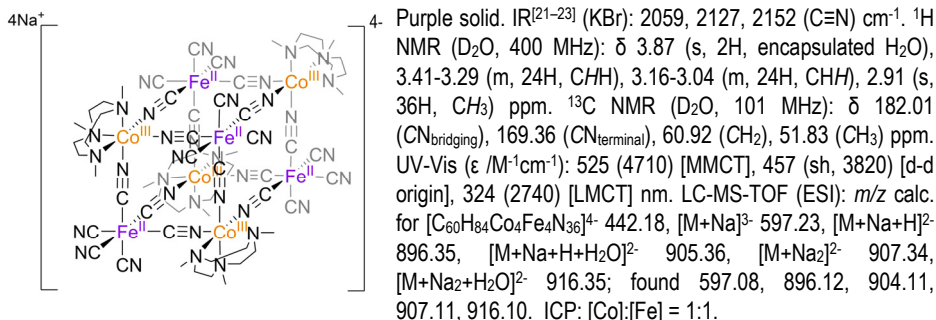
[Co<sup>III</sup>(Me<sub>3</sub>TACN)Cl<sub>3</sub>] (0.24 g, 0.7 mmol) was dissolved in 100 cm<sup>3</sup> of water and pH was adjusted to 8-9 while the colour of the solution changes from dark blue to purple due to Cl<sup>-</sup> to OH<sup>-</sup> substitution. Then, 1.1 g (2.2 mmol) of Na<sub>4</sub>[Fe(CN)<sub>6</sub>]·10H<sub>2</sub>O dissolved in 30 cm<sup>3</sup> of water, was slowly added. The solution became almost immediately dark blue/green and was left to react at 60 °C for 18 h, checking that pH was maintained during the first hours.

The final purple solution contained some brown precipitate that was filtered and discarded; the filtrate was taken to dryness in a rotary evaporator obtaining a purple solid.

This solid was dissolved in the minimum quantity of water and was chromatographed with a Sephadex G-25M Column (mass exclusion chromatography). Three fractions were obtained: the first one was brown/black with a broad band in UV-Vis between 400-600 nm (discarded as a polymer), the second was a purple well-defined band and contains most of our product, and the last one was characterised as free hexacyanidoferrate(II).

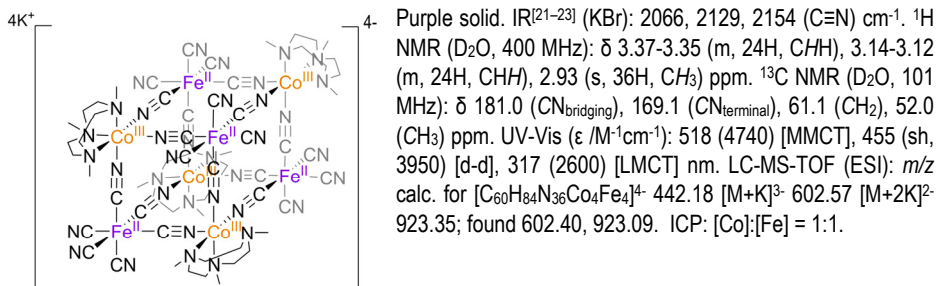
For further purification, the purple fraction was diluted to 500 cm<sup>3</sup> and was chromatographed with a Sephadex DEAE (anionic exchange). On the top of the column remained the rest of the inorganic polymers and the desired product was eluted with aqueous 0.2 M NaClO<sub>4</sub>. Any remaining hexacyanidoferrate was finally eluted with 0.4 M NaClO<sub>4</sub>. The excess of sodium perchlorate was removed by concentrating our final solution and passing it through the

Sephadex G-25M column several times. Finally, the solution was taken to dryness and a purple solid was obtained.



#### 5.2.4. Synthesis of K<sub>4</sub>{[Co<sup>III</sup>(Me<sub>3</sub>TACN)]<sub>4</sub>{(μ-NC)<sub>3</sub>Fe<sup>II</sup>(CN)<sub>6</sub>]<sub>4</sub>} (K-Cube)

The K-Cube was prepared following the same procedure as described for the Na-Cube using the corresponding potassium salts.



#### 5.3. PREPARATION OF FULLY OXIDIZED CUBE {[Co<sup>III</sup>(Me<sub>3</sub>TACN)]<sub>4</sub>{(μ-NC)<sub>3</sub>[Fe<sup>III</sup>(CN)<sub>6</sub>]<sub>4</sub>}

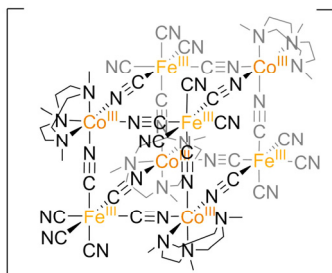
A solution of 0.1 g (54 μmol) of Na-Cube in 40 cm<sup>3</sup> of water (purple colour) and a 60 cm<sup>3</sup> solution of 15 g (0.063 mol) of Na<sub>2</sub>S<sub>2</sub>O<sub>8</sub> were mixed and left to react at room temperature overnight.

The final solution turned yellow and had some finely suspended precipitate which was filtered and discarded with two Whatman N°2 paper filters. The yellow solution was taken to dryness (UV-Vis: 439 nm). And the pale-yellow solid obtained, corresponding to our product,

was filtered with N°4 filter crucible. Adding some drops of water to the solid produced intense yellow mother liquor while the precipitate became white, corresponding to most of the oxidant added. The mother liquor was taken to dryness with a rotary evaporator and an off-yellow solid was obtained. This process was repeated two more times to eliminate as much as possible the excess of oxidant from the oxidized sample.

The crude solid was dissolved in 10 cm<sup>3</sup> of water and chromatographed with a Sephadex G-25M (size exchange) chromatography column. Initially, a very good separation of three bands was observed: the first was purple, corresponding to reduced Cube that was not reacted, the second was green, that corresponded to an inorganic polymer, and the third was yellow corresponding to the desired product, the fully oxidized Cube. Water was passed and, on elution through the column, the green and yellow bands became purple.

Three purple fractions and a yellower one were obtained, but after 2h, the first fraction and the second were still purple while the third had obtained a mixed colour of purple and yellow, and the fourth had turned completely yellow. The fourth band was assumed as the fully oxidised product and its characterization was carried out.



Yellow solid. UV-Vis: 440 nm [LMCT]. ICP: [Co]:[Fe] = 1:1  
LC-MS-TOF (ESI):  $m/z$  calc. for  $[C_{60}H_{84}Co_4Fe_4N_{36}+Na+H_2O]^+$   
1809.7; found 1809.1

Paramagnetic.

## 5.4. KINETICS OF THE OXIDATION OF CUBE

### 5.4.1. Preparation of Buffers<sup>[24]</sup>

Borax buffer [pH = 8.2,  $I = 1.0$  M (NaClO<sub>4</sub>)] was prepared by dissolving 8.09 g (0.04 mol) Na<sub>2</sub>B<sub>4</sub>O<sub>7</sub> and 54.66 g (0.38 mol) of NaClO<sub>4</sub>·H<sub>2</sub>O in 420 cm<sup>3</sup> of distilled water. The pH was adjusted to 8.2 with NaOH 0.1 M and HClO<sub>4</sub> 1.0 M.

HClO<sub>4</sub> [ $I = 1.0$  M (NaClO<sub>4</sub>)] was used as a buffer by excess for the kinetics at pH 0-1. A 1.0 M solution (pH approx. 0) was prepared by diluting 19.5 cm<sup>3</sup> of a 2.5424 M standard solution.

Another one 0.5 M (pH approx. 0.3) was prepared by dissolving 0.76 g (5.4 mmol) of  $\text{NaClO}_4 \cdot \text{H}_2\text{O}$  in 5  $\text{cm}^3$  of the previously prepared 1.0 M solution and adding water to 10  $\text{cm}^3$ . A 0.1 M solution of  $\text{HClO}_4$  (pH approx. 1) was also prepared following the same procedure, with 1.27 g (9.0 mmol) of  $\text{NaClO}_4 \cdot \text{H}_2\text{O}$  and 1  $\text{cm}^3$  of the 1.0 M solution.

#### 5.4.2. Preparation of stock solutions of the reactants

A stock solution 1.2 mM of Na-Cube and another one 10 mM of K-Cube were prepared, the concentrations were determined approximately by the extinction coefficient observed in UV-Vis.

Stock solutions of the oxidizing agent were prepared, for the kinetic study at pH 8.2 by dissolving necessary amounts of  $\text{Na}_2\text{S}_2\text{O}_8$  in the borax buffer to a final concentration of 0.075 M and 0.5 M, and other solutions 1.0 M, 2.0M and 2.3M of  $\text{Na}_2\text{S}_2\text{O}_8$  in water were prepared for the study at acidic pH.

#### 5.4.3. Oxidation reaction

The kinetic runs at high pH were conducted under pseudo-first-order conditions by mixing 0.06  $\text{cm}^3$  of the stock solution of the corresponding Cube (final concentration of Na-Cube in the cell = 28.8  $\mu\text{M}$ ) with an excess of stock solutions of  $\text{Na}_2\text{S}_2\text{O}_8$  to obtain concentrations of  $\text{S}_2\text{O}_8^{2-}$  between 0.048M and 0.4M. Finally, the total volume of the cell was adjusted to 2.5  $\text{cm}^3$  adding the necessary volumes of the Borax buffer.

The kinetic studies at low pHs were made by mixing 0.03  $\text{cm}^3$  of the stock solution of Na-Cube (final concentration = 17.7  $\mu\text{M}$ ) with the calculated amounts of stock solutions of  $\text{Na}_2\text{S}_2\text{O}_8$  to obtain concentrations of  $[\text{S}_2\text{O}_8]^{2-}$  between 2.5 mM and 30 mM. The total volume of the cell was adjusted to 2.0  $\text{cm}^3$  adding the necessary volumes of the corresponding solution of  $\text{HClO}_4$  for each pH studied.

All kinetic runs were carried out under pseudo-first-order conditions and the kinetic time-resolved profiles for the reactions were obtained by an Agilent G1103A UV-Vis spectrophotometer or a Varian Cary 50 Bio UV-Vis spectrophotometer, both connected to a Julabo F25 thermostatic bath. Data were collected by measuring absorption from 300 to 800 nm at 25°C at different time ranges and intervals.

Data obtained of the observed rate constants  $k_{\text{obs}}(\text{s}^{-1})$  from the 3D kinetic spectrum (Absorbance-Wavelength-Time), studied under first-order concentrations conditions, was

treated with Specfit32 software.<sup>[25]</sup> This program allow the time-resolved data to be fitted under pseudo-first-order conditions to a ( $A \rightarrow B$   $k_{\text{obs}1}$ ,  $B \rightarrow C$   $k_{\text{obs}2}$ ,  $C \rightarrow D$   $k_{\text{obs}3}$ ,  $D \rightarrow E$   $k_{\text{obs}4}$ ) or, if necessary, a ( $A \rightarrow B$   $k_{\text{obs}1}$ ,  $B \rightarrow C$   $k_{\text{obs}2}$ ,  $C \rightarrow D$   $k_{\text{obs}3}$ ) models, depending on which better fitted Absorbance-Time traces of the UV-Vis spectrums recorded, thus producing an observed rate-constants for each experiment.

Three or four observed rate-constants ( $k_{\text{obs}}$ ) were obtained in each concentration of oxidant (All values are collected in Appendix 1). Then, the dependence of these values of  $k_{\text{obs}}$  with different concentration of oxidant was conducted with OriginPro 8 software to fit to the proper equation and to obtain the  $K_{\text{OS}}$  and  $k_{\text{ox}}$  of each rate step.

## 6. RESULTS AND DISCUSSION

### 6.1. SYNTHESIS OF CUBE

The Cube was prepared following the procedure described in the experimental part. By this method used, the Cube prepared with sodium salts always has impurities of sodium perchlorate which are difficult to eliminate if not passed many times by a Sephadex G-25M chromatography column. In the case of the Cube prepared with potassium salts, this problem is presented with salts of potassium chloride that should be eliminated by the same method or taking advantage of the fact that the Cube is soluble in methanol and the KCl is not. It could be dissolved in methanol in order to remove most of the KCl from the product.

The two Cubes prepared were expected to be equal, but when they were characterized, it was observed that in their  $^1\text{H-NMR}$  and  $^{13}\text{C-NMR}$  the signals do not appear in the same place. In the  $^1\text{H-NMR}$ , in both cases, there was a singlet that integrated the protons of  $\text{Me}_3\text{TACN}$  methyls and two doublets of doublets corresponding to  $\text{CH}_2$  of  $\text{Me}_3\text{TACN}$  where the H were chemically equivalent but not magnetically equivalent. In addition, the Cube prepared with sodium salts showed an extra signal that integrated two H's and did not correspond to the geometry of the Cube. No other unexpected signals were observed in the  $^{13}\text{C-NMR}$ , so it was thought that the Na-Cube encapsulates a water molecule in its structure.

In the mass spectrum, the observed peaks in MS at 905.36 and 916.35 m/z confirmed that an  $\text{H}_2\text{O}$  molecule was encapsulated into the Na-Cube while the Cube prepared with potassium salts, K-Cube, had no peaks in its Mass spectroscopy that indicate this phenomenon. This fact could be explained because of a different self-assembly mechanism depending on the cation size of the salts used as reactive.

### 6.2. PREPARATION OF OXIDIZED CUBE

First oxidation of the sodium Cube at neutral pH was performed with an excess of 1200 fold more peroxodisulfate than Cube. It was seen that, when passing through the column, when the remains of peroxodisulfate in the sample were eliminated, the oxidized Cube was reduced

again. It was observed that under not very acidic conditions or with a low excess of the oxidizing agent, the oxidized Cube could not be obtained because, in an aqueous medium, it reverts to the original  $\text{Co}^{\text{III}}/\text{Fe}^{\text{II}}$  reduced form of the complex.

In a second oxidation, the fully oxidized Cube only could be obtained impure with an excess of peroxodisulfate. In any other case, it has been confirmed that it returns to the completely reduced form if the pH is not acidic or if there is no excess of the oxidant.

### 6.3. MODELLING THE TIME-RESOLVED SPECTRAL CHANGES

This type of mixed-valence complexes presents a wide range of colour changes based on the oxidation states of the metal. In this case, two types of transitions were identified as being responsible of colour: MMCT between  $\text{Fe}^{\text{II}}$  and  $\text{Co}^{\text{III}}$  in the reduced Cube (purple), and LMCT between  $\text{CN}^-$  ligand and  $\text{Fe}^{\text{III}}$  in the oxidized Cube (yellow).

The oxidation of the Cube by peroxodisulfate was studied under the conditions mentioned in the experimental section.

Other buffers were tried, like HEPES<sup>[24]</sup> [pH 7 /  $I = 1.0 \text{ M}$  ( $\text{NaClO}_4$ )], but were not used because  $\text{Na}_2\text{S}_2\text{O}_8$ , used as the oxidant, oxidizes the buffer and the solution of oxidizing agent turns yellow. As the study was to be carried out by measuring absorbance in the UV-Vis zone, oxidizing solutions used should not absorb in this wavelength range.

The processes were studied with  $\text{S}_2\text{O}_8^{2-}$  as oxidant and were found to produce well-behaved first-order absorbance vs time traces in the acidic pH range. When the pH value was increased (borax conditions), the spectral changes became more erratic; no reliable values of  $k_{\text{obs}}$  could be obtained. Under these conditions, the redox reactions were observed to revert with time to the original  $\text{Co}^{\text{III}}/\text{Fe}^{\text{II}}$  reduced form of the complex, which implied that all the oxidizing agent had been consumed in a catalytic process and the reduction reaction had taken place. This (reverse) reduction reaction became also dominant when the concentration of peroxodisulfate was low because the reduction reaction takes place in an aqueous medium.

For this reason, the reactions with low peroxodisulfate concentrations seemed to be so slow, and a very large excess (1000-2000 times more than Cube) was needed in order to force the oxidation of the Cube and overcome this regression in the reaction.

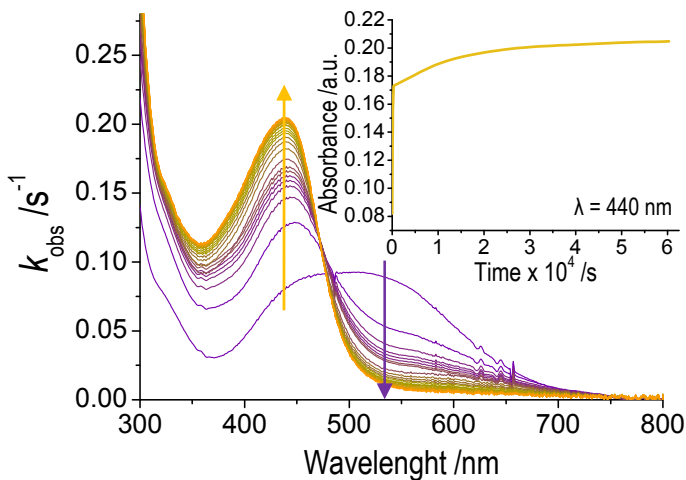


Figure 4. UV-Vis spectral changes obtained for the oxidation reaction of Na-Cube with an excess of 1700 fold  $\text{S}_2\text{O}_8^{2-}$ . Borax buffer. ( $T = 25\text{ }^\circ\text{C}$ ,  $\text{pH} = 8.2$ ,  $I = 1.0\text{ M}$  ( $\text{NaClO}_4$ ),  $[\text{Na-Cube}] = 2.88 \times 10^{-5}\text{ M}$ ,  $[\text{S}_2\text{O}_8^{2-}] = 4.8 \times 10^{-2}\text{ M}$ ).

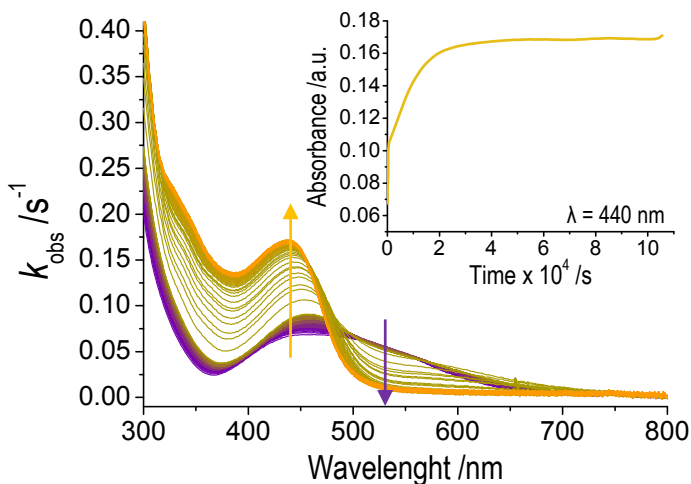


Figure 5. UV-Vis spectral changes obtained for the oxidation reaction of K-Cube with an excess of 1700 fold  $\text{S}_2\text{O}_8^{2-}$ . Borax buffer. ( $T = 25\text{ }^\circ\text{C}$ ,  $\text{pH} = 8.2$ ,  $I = 1.0\text{ M}$  ( $\text{NaClO}_4$ ),  $[\text{K-Cube}] = 2.39 \times 10^{-4}\text{ M}$ ,  $[\text{S}_2\text{O}_8^{2-}] = 4.0 \times 10^{-1}\text{ M}$ ).

As seen in Figures 4 and 5, the K-Cube gets to its fully oxidized form faster than Na-Cube with peroxodisulfate at pH 8.2. The reaction with an excess of 1700 fold peroxodisulfate than

Cube at 440 nm, the K-Cube ceased to evolve in 48000 s (approx. 13 h) and the Na-Cube needed at least 62000 s (approx. 17h) to stop changing in the same conditions.

In all conditions studied, different pH and different concentration of peroxodisulfate, it was observed an increase in the absorbance around 440 nm, which corresponds to the appearance of the oxidized Cube (LMCT, ligand-to-metal charge transition between CN and Fe<sup>III</sup>), and a decrease of the broad maximum around 540 nm, which corresponds to the waste of the fully reduced Cube (MMCT Fe<sup>II</sup> to Co<sup>III</sup>).

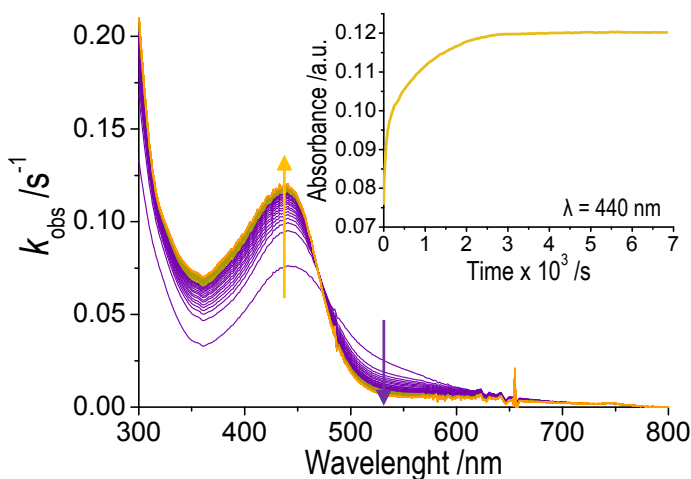


Figure 6. UV-Vis spectral changes obtained for the oxidation reaction of Na-Cube with an excess of 1700 fold  $S_2O_8^{2-}$ .  $HClO_4$  buffer. (T = 25 °C, pH = 0.3, I = 1.0 M ( $NaClO_4$ ),  $[Na-Cube] = 1.77 \times 10^{-5}$  M,  $[S_2O_8^{2-}] = 3.0 \times 10^{-2}$  M).

As said previously, when the oxidizing agent was consumed, takes place the reduction reaction with the OH<sup>-</sup> of the medium producing H<sub>2</sub>O<sub>2</sub>, but a decrease in the absorbance at 440 nm (disappearance of oxidized Cube) or an increase at 540 nm (formation of reduced Cube) was not observed. This could be explained because of a catalytic process, the high excess of oxidant in the cell quickly oxidize again the reduced Cube. It could be confirmed because, as seen in Figure 6, the oxidation reaction at acidic pH was “faster” (approx. 1.5h) than in higher pH, and all results obtained for the different concentrations of peroxodisulfate were clearer. It makes sense because, at acidic pH, the oxidation reaction could overcome the reduction reaction because there is less concentration of hydroxide ions in the solution.

## 6.4. STUDY AND INTERPRETATION OF THE EFFECT OF pH AND CONCENTRATION OF $[S_2O_8]^{2-}$

Reactions were followed by UV-vis spectroscopy in the full 300-800 nm range. Observed rate constants were derived from the absorbance vs time traces at wavelengths where a maximum increase (approx. 440 nm) or decrease (approx. 540 nm) of absorbance was observed. In all cases, pseudo-first-order conditions were maintained, and the complex concentration was kept at  $(17-29) \times 10^{-6}$  M.

In the course of this oxidation study, the process has been found to behave in a reversible way at high pH values, indicating that the oxidized form of the complex  $[(Co^{III}(Me_3TACN)_4)\{\mu-N(C)_3[Fe^{III}(CN)_6]_4\}]$  is an oxidant of water producing hydrogen peroxide. Due to this, the study has only been carried out at acidic pH.

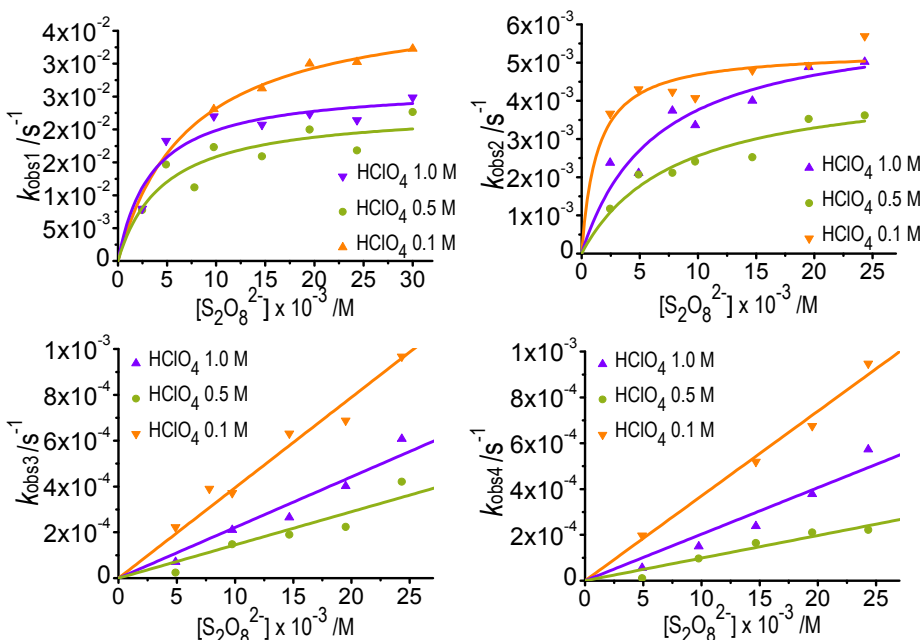


Figure 7. Plot of the values of the pseudo-first-order rate constants, a)  $k_{obs1}$ , b)  $k_{obs2}$ , c)  $k_{obs3}$ , d)  $k_{obs4}$ , vs.  $[S_2O_8^{2-}]$  for the oxidation of Na-Cube at different  $[HClO_4]$  ( $\blacktriangle$  purple 1.0 M,  $\bullet$  green 0.5 M,  $\blacktriangledown$  orange 0.1 M).

In order to determine the mechanism of the oxidation reaction, the kinetics trend of the observed pseudo-first-order rate constants obtained with Specfit32 software, as indicated in the experimental part, was treated with OriginPro8 software (Figure 7). Depending on the curvature

on the plots generated by this program,  $k_{\text{obs}}$  rate constants could show a typical limiting behaviour for outer-sphere redox processes, and be represented by Equation 1a, where the formation of the precursor outer-sphere complex ( $K_{\text{OS}}$ ) was dominant. Or, if not, the observed rate constant showed a linear dependence with the peroxodisulfate concentration and its tendency was described by Equation 1b.

$$\text{a) } k_{\text{obs}} = \frac{K_{\text{OS}}k_{\text{ox}}[\text{S}_2\text{O}_8^{2-}]}{1 + K_{\text{OS}}[\text{S}_2\text{O}_8^{2-}]} \quad \text{b) } k_{\text{obs}} = K_{\text{OS}}k_{\text{ox}}[\text{S}_2\text{O}_8^{2-}]$$

Equation 1. Rate law for the outer-sphere oxidation process.

Observing Figure 7, while  $k_{\text{obs}1}$  and  $k_{\text{obs}2}$  produced a rate law such as that indicated in Equation 1a,  $k_{\text{obs}3}$  and  $k_{\text{obs}4}$  produced another rate law such as that indicated in Equation 1b. These results indicate that for the oxidation of  $\{\text{Co}^{\text{III}}/\text{Fe}^{\text{II}}\}_4^{4+}$  to  $\{\text{Co}^{\text{III}}_4/\text{Fe}^{\text{II}}_3\text{Fe}^{\text{III}}\}^{3-}$  ( $k_{\text{obs}1}$ ) and this to  $\{\text{Co}^{\text{III}}_4/\text{Fe}^{\text{II}}_2\text{Fe}^{\text{III}}_2\}^{2-}$  ( $k_{\text{obs}2}$ ), a limiting outer-sphere precursor formation was observed, where the formation of the precursor outer-sphere complex ( $K_{\text{OS}}$ ) was dominant. And for the reaction of  $\{\text{Co}^{\text{III}}_4/\text{Fe}^{\text{II}}_2\text{Fe}^{\text{III}}_2\}^{2-}$  to  $\{\text{Co}^{\text{III}}_4/\text{Fe}^{\text{II}}\text{Fe}^{\text{III}}_3\}^{-}$  ( $k_{\text{obs}3}$ ) and from this one to fully oxidized Cube,  $\{\text{Co}^{\text{III}}/\text{Fe}^{\text{III}}\}_4$  ( $k_{\text{obs}4}$ ), these outer-sphere complex and its equilibrium constant were not relevant.

In Table 1, are detailed all outer-sphere complex equilibrium constants and oxidation rate constants obtained from the fitting of  $k_{\text{obs}}$  shown in Figure 7.

| [HClO <sub>4</sub> ]<br>/M | $K_{\text{OS}1}$<br>/s <sup>-1</sup> | $k_{\text{ox}1}$<br>(x 10 <sup>-3</sup> ) /s <sup>-1</sup> | $K_{\text{OS}2}$<br>/s <sup>-1</sup> | $k_{\text{ox}2}$<br>(x 10 <sup>-3</sup> ) /s <sup>-1</sup> | $K_{\text{OS}3} \times k_{\text{ox}3}$<br>(x 10 <sup>-3</sup> ) /s <sup>-1</sup> | $K_{\text{OS}4} \times k_{\text{ox}4}$<br>(x 10 <sup>-3</sup> ) /s <sup>-1</sup> |
|----------------------------|--------------------------------------|--|--------------------------------------|--|--|--|
| 1                          | 300 ± 100                            | 27 ± 2   | 160 ± 60                             | 6.2 ± 0.8  | 22 ± 1   | 20 ± 2   |
| 0.5                        | 200 ± 100                            | 23 ± 3   | 120 ± 40                             | 4.6 ± 0.6  | 14 ± 1   | 99 ± 0.7   |
| 0.1                        | 140 ± 20                             | 40 ± 2   | 700 ± 300                            | 5.3 ± 0.3  | 39 ± 2   | 37 ± 1   |

(a)  $k_{\text{obs}1}$  and  $k_{\text{obs}2}$  were fitted following Equation 1a.

(b)  $k_{\text{obs}3}$  and  $k_{\text{obs}4}$  were fitted following Equation 1b.

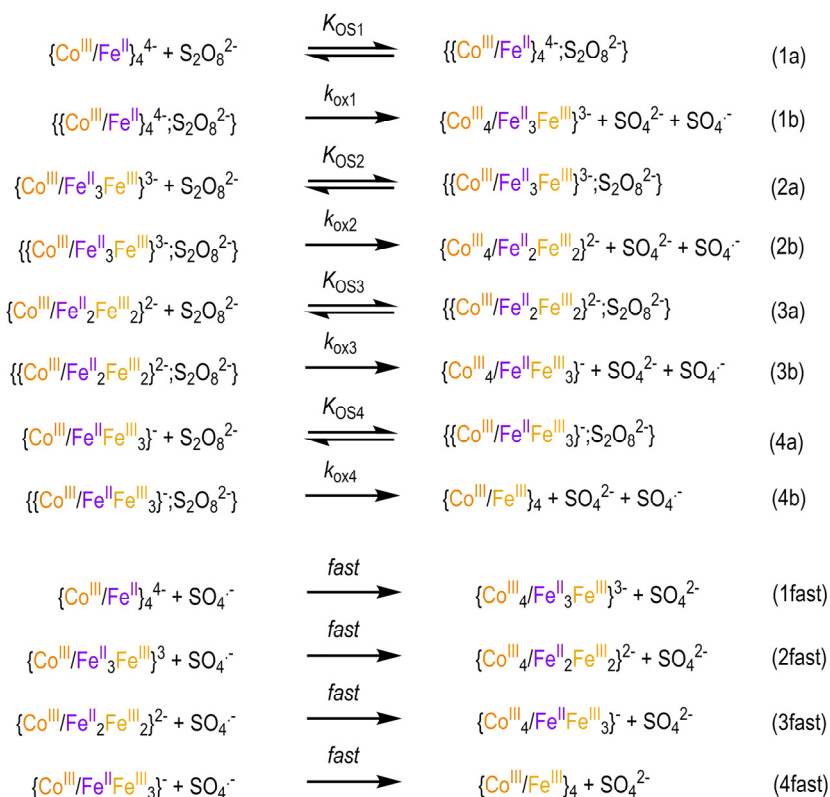
Table 1. Kinetic parameters for the reaction steps observed in the oxidation of the Na-Cube with  $\text{S}_2\text{O}_8^{2-}$  at different concentration of HClO<sub>4</sub>.

For the third and fourth reaction, the slope of the linear dependence of the  $k_{\text{obs}}$  values corresponds to  $K_{\text{OS}} \times k_{\text{ox}}$  as indicated in Equation 1b and could not be obtained separately.

## 6.5. REDOX MECHANISM

### 6.5.1. Oxidation reaction

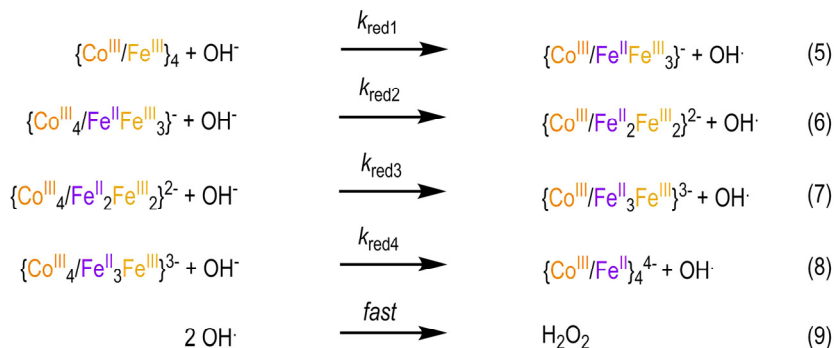
According to the reactivity observed for the compounds with lower nuclearity previously prepared,<sup>[17,18]</sup> and the results obtained in the kinetic study, an outer-sphere mechanism to the oxidation of  $\{[Co^{III}(Me_3TACN)_4\{\mu-NC\}_3\{Fe^{II}(CN)_6\}_4\}^{4-}$  ( $\{Co^{III}/Fe^{II}\}_4^{4-}$ , Cube) with peroxodisulfate was proposed as described in Scheme 2. Where the reactions 3a and 4a were found to be an equilibrium not significantly shifted to the outer-sphere precursor formation, the values of  $K_{OS3}$  and  $K_{OS4}$  were not relevant.



Scheme 2. Outer-sphere oxidation mechanism of Cube with peroxodisulfate.

### 6.5.2. Reduction reaction

As seen in the mechanism of the reduction reaction of Square complex,<sup>[18]</sup> and according to the changes observed during the preparation of the oxidized Cube, the mechanism to reduce fully oxidized Cube with OH<sup>-</sup> was proposed to be similar as described in Scheme 3. This could explain why the fully oxidized Cube was difficult to obtain in an aqueous medium without an excess of peroxodisulfate.



Scheme 3. Reduction mechanism of fully oxidized Cube with OH<sup>-</sup>.

## 7. CONCLUSIONS

Two new compounds of cyanido-bridged mixed-valence with cubic shape,  $[\{Co^{III}(Me_3TACN)\}_4\{\mu\text{-NC}\}_3\{Fe^{II}(CN)_6\}_4]^{4-}$ , have been synthesized and characterized. One prepared with sodium salts (Na-Cube) that seems to encapsulate an  $H_2O$  in its structure, while the other, prepared with potassium salts (K-Cube), do not have this  $H_2O$  encapsulated.

The fully oxidized form of the Cube has been obtained from the oxidation of the reduced Na-Cube with peroxodisulfate. Even at slightly acidic conditions, it has been observed that, without a presence of an excess of the oxidant, the oxidized Cube revert to the original form, oxidizing the water in the medium and producing  $H_2O_2$  in a catalytic process.

The kinetic study of the four-step oxidation reaction of the  $[\{Co^{III}(Me_3TACN)\}_4\{\mu\text{-NC}\}_3\{Fe^{II}(CN)_6\}_4]^{4-}$  Cubes, by peroxodisulfate in different pH solutions at 25 °C, have been conducted under pseudo-first-order conditions and a mechanism of the oxidation reaction of the Cube have been described as two first step that requires the existence of an equilibrium process prior to the rate-determining step, and two last steps where this equilibrium was not relevant.



## 8. REFERENCES AND NOTES

- (1) Robin, M. B.; Day, P. *Adv. Inorg. Chem. Radiochem.* **1967**, *10*, 247.
- (2) Sykes, A. G. *Adv. Inorg. Chem. Radiochem.* **1968**, *10*, 153.
- (3) Bernhardt, P. V.; Martínez, M.; Rodríguez, C. *Inorg. Chem.* **2009**, *48*, 4787.
- (4) Alcázar, L.; Aullón, G.; Ferrer, M.; Martínez, M. *Chem. – A Eur. J.* **2016**, *22*, 15227.
- (5) Jiménez, J. R.; Tricoire, M.; Garnier, D.; Chamoreau, L. M.; Von Bardeleben, J.; Journaux, Y.; Li, Y.; Lescouëzec, R. *Dalton Trans.* **2017**, *46*, 15549.
- (6) Bernhardt, P. V.; Martínez, M. *Inorg. Chem.* **1999**, *38*, 424.
- (7) Bernhardt, P. V.; Macpherson, B. P.; Martínez, M. *Inorg. Chem.* **2000**, *39*, 5203.
- (8) Bernhardt, P. V.; Macpherson, B. P.; Martínez, M. *J. Chem. Soc. Dalton Trans.* **2002**, 1435.
- (9) Bernhardt, P. V.; Bozoglian, F.; Macpherson, B. P.; Martínez, M.; González, G.; Sienna, B. *Eur. J. Inorg. Chem.* **2003**, 2512.
- (10) Lescouëzec, R.; Vaissermann, J. et al. *Angew. Chem. Int. Ed.* **2003**, *42*, 1433.
- (11) Bernhardt, P. V.; Bozoglian, F.; Macpherson, B. P.; Martínez, M. *Coord. Chem. Rev.* **2005**, *249*, 1902.
- (12) Bernhardt, P. V.; Bozoglian, F.; González, G.; Martínez, M.; Macpherson, B. P.; Sienna, B. *Inorg. Chem.* **2006**, *45*, 74.
- (13) Bozoglian, F. *Sistemas discretos de valencia mixta Co/Fe: síntesis, caracterización y estudio cinético-mecanístico de sus reacciones redox.*, Universitat de Barcelona, 2006.
- (14) Allen, G. C.; Hush, N. S. *Prog. Inorg. Chem.* **1967**, 357.
- (15) Hush, N. S. *Prog. Inorg. Chem.* **1967**, 391.
- (16) Rosseinsky, D. R.; Mortimer, R. J. *Adv. Mater.* **2001**, *13*, 783.
- (17) Bernhardt, P. V.; Bozoglian, F.; Macpherson, B. P.; Martínez, M.; Merbach, A. E.; González, G.; Sienna, B. *Inorg. Chem.* **2004**, *43*, 7187.
- (18) Alcázar, L.; Bernhardt, P. V.; Ferrer, M.; Font-Bardia, M.; Gallen, A.; Jover, J.; Martínez, M.; Peters, J.; Zerk, T. J. *Inorg. Chem.* **2018**, *57*, 8465.
- (19) Searle, G. H.; Wang, D.-N.; Larsen, S.; Larsen, E. *Acta Chem. Scand.* **1992**, *46*, 38.
- (20) AlQaradawi, S. Y.; Bazzi, H. S.; Mostafa, A.; Nour, E.-M. *Spectrochim. Acta Part A Mol. Biomol. Spectrosc.* **2008**, *71*, 1594.
- (21) Nakamoto, K. *Infrared and Raman spectra of inorganic and coordination compounds*, 6th ed.; Wiley: New York, 2009.

- 
- (22) Pretsch, E.; Clerc, T.; Seibl, J.; Simon, W. *Tablas para la elucidación estructural de compuestos orgánicos por métodos espectroscópicos*; Alhambra, 1980; Vol. 44.
- (23) Posición de las bandas de absorción correspondientes de Grupos orgánicos o inorgánicos. <http://www.ehu.es/imacris/PIE06/web/tablasIR.htm> (accessed Mar 19, 2019).
- (24) Good, N. E.; Winget, G. D.; Winter, W.; Connolly, T. N.; Izawa, S.; Singh, R. M. M. *Biochemistry* **1966**, 5, 467.
- (25) Binstead, R. A.; Zuberbuhler, A. D.; Jung, B. *SPECFIT32 [3.0.34]*; Spectrum Software Associates: Marlborough, MA, 2005.

# APPENDICES



## APPENDIX 1: KINETIC DATA

| pH                                 | [S <sub>2</sub> O <sub>8</sub> <sup>2-</sup> ] /M | k <sub>obs1</sub> /s <sup>-1</sup> | k <sub>obs2</sub> /s <sup>-1</sup> | k <sub>obs3</sub> /s <sup>-1</sup> | k <sub>obs4</sub> /s <sup>-1</sup> |
|------------------------------------|---|------------------------------------|------------------------------------|------------------------------------|------------------------------------|
| <b>8.2 (a)</b>                     | 48 x 10 <sup>-3</sup>                             | 2.9 x 10 <sup>-2</sup>             | 2.6 x 10 <sup>-3</sup>             | 1.6 x 10 <sup>-4</sup>             | 4.5 x 10 <sup>-5</sup>             |
| <b>(Borax 0.1 M)</b>               | 53 x 10 <sup>-3</sup>                             | 3.1 x 10 <sup>-2</sup>             | 1.2 x 10 <sup>-2</sup>             | 1.7 x 10 <sup>-4</sup>             | 4.4 x 10 <sup>-5</sup>             |
| <b>I = 1 M (NaClO<sub>4</sub>)</b> | 58 x 10 <sup>-3</sup>                             | 2.8 x 10 <sup>-2</sup>             | 3.2 x 10 <sup>-3</sup>             | 2.1 x 10 <sup>-4</sup>             | 5.1 x 10 <sup>-5</sup>             |
|                                    | 63 x 10 <sup>-3</sup>                             | 2.5 x 10 <sup>-2</sup>             | 3.2 x 10 <sup>-3</sup>             | 1.7 x 10 <sup>-4</sup>             | 3.3 x 10 <sup>-5</sup>             |
|                                    | 68 x 10 <sup>-3</sup>                             | 4.2 x 10 <sup>-2</sup>             | 6.5 x 10 <sup>-3</sup>             | 2.2 x 10 <sup>-4</sup>             | 3.4 x 10 <sup>-5</sup>             |
|                                    | 73 x 10 <sup>-3</sup>                             | 3.0 x 10 <sup>-2</sup>             | 8.5 x 10 <sup>-3</sup>             | 1.8 x 10 <sup>-4</sup>             | 3.9 x 10 <sup>-5</sup>             |
|                                    | 80 x 10 <sup>-3</sup>                             | 3.6 x 10 <sup>-2</sup>             | 1.1 x 10 <sup>-3</sup>             | 2.5 x 10 <sup>-4</sup>             | 2.0 x 10 <sup>-5</sup>             |
|                                    | 11 x 10 <sup>-2</sup>                             | 2.4 x 10 <sup>-2</sup>             | 2.3 x 10 <sup>-3</sup>             | 2.0 x 10 <sup>-4</sup>             | 2.9 x 10 <sup>-5</sup>             |
|                                    | 14 x 10 <sup>-2</sup>                             | 3.3 x 10 <sup>-2</sup>             | 3.8 x 10 <sup>-3</sup>             | 4.3 x 10 <sup>-4</sup>             | 7.9 x 10 <sup>-5</sup>             |
|                                    | 17 x 10 <sup>-2</sup>                             | 2.7 x 10 <sup>-2</sup>             | 5.3 x 10 <sup>-3</sup>             | 1.5 x 10 <sup>-4</sup>             | 1.4 x 10 <sup>-5</sup>             |
|                                    | 20 x 10 <sup>-2</sup>                             | 2.6 x 10 <sup>-2</sup>             | 4.5 x 10 <sup>-3</sup>             | 3.3 x 10 <sup>-4</sup>             | 1.2 x 10 <sup>-5</sup>             |
|                                    | 22 x 10 <sup>-2</sup>                             | 2.7 x 10 <sup>-2</sup>             | 5.3 x 10 <sup>-3</sup>             | 4.5 x 10 <sup>-4</sup>             | 1.5 x 10 <sup>-4</sup>             |
|                                    | 25 x 10 <sup>-2</sup>                             | 2.8 x 10 <sup>-2</sup>             | 6.7 x 10 <sup>-3</sup>             | 3.1 x 10 <sup>-4</sup>             |                                    |
|                                    | 30 x 10 <sup>-2</sup>                             | 2.8 x 10 <sup>-2</sup>             | 4.1 x 10 <sup>-3</sup>             | 3.3 x 10 <sup>-4</sup>             |                                    |
|                                    | 35 x 10 <sup>-2</sup>                             | 2.4 x 10 <sup>-2</sup>             | 1.5 x 10 <sup>-3</sup>             | 3.9 x 10 <sup>-4</sup>             |                                    |
|                                    | 40 x 10 <sup>-2</sup>                             | 2.7 x 10 <sup>-2</sup>             | 3.2 x 10 <sup>-3</sup>             | 4.5 x 10 <sup>-4</sup>             |                                    |
| <b>8.2 (b)</b>                     | 48 x 10 <sup>-3</sup>                             | 1.1 x 10 <sup>-1</sup>             | 2.8 x 10 <sup>-3</sup>             |                                    |                                    |
| <b>(Borax 0.1 M)</b>               | 58 x 10 <sup>-3</sup>                             | 7.2 x 10 <sup>-2</sup>             | 1.9 x 10 <sup>-3</sup>             | 1.3 x 10 <sup>-4</sup>             | 1.1 x 10 <sup>-5</sup>             |
| <b>I = 1 M (NaClO<sub>4</sub>)</b> | 63 x 10 <sup>-3</sup>                             | 8.9 x 10 <sup>-2</sup>             | 7.8 x 10 <sup>-4</sup>             | 8.7 x 10 <sup>-5</sup>             | 9.2 x 10 <sup>-6</sup>             |
|                                    | 68 x 10 <sup>-3</sup>                             | 5.0 x 10 <sup>-2</sup>             | 3.0 x 10 <sup>-3</sup>             | 1.2 x 10 <sup>-4</sup>             | 1.3 x 10 <sup>-5</sup>             |
|                                    | 80 x 10 <sup>-3</sup>                             | 4.2 x 10 <sup>-2</sup>             | 1.8 x 10 <sup>-3</sup>             | 1.1 x 10 <sup>-4</sup>             | 3.7 x 10 <sup>-6</sup>             |
|                                    | 11 x 10 <sup>-2</sup>                             | 2.9 x 10 <sup>-2</sup>             | 1.6 x 10 <sup>-5</sup>             |                                    |                                    |
|                                    | 17 x 10 <sup>-2</sup>                             | 2.4 x 10 <sup>-2</sup>             | 1.5 x 10 <sup>-4</sup>             | 1.7 x 10 <sup>-4</sup>             | 4.8 x 10 <sup>-6</sup>             |
|                                    | 20 x 10 <sup>-2</sup>                             | 4.7 x 10 <sup>-2</sup>             | 1.4 x 10 <sup>-3</sup>             | 2.6 x 10 <sup>-4</sup>             | 1.6 x 10 <sup>-5</sup>             |
|                                    | 22 x 10 <sup>-2</sup>                             | 9.6 x 10 <sup>-2</sup>             | 3.5 x 10 <sup>-3</sup>             | 2.1 x 10 <sup>-4</sup>             | 7.5 x 10 <sup>-6</sup>             |
|                                    | 25 x 10 <sup>-2</sup>                             | 9.0 x 10 <sup>-2</sup>             | 2.4 x 10 <sup>-3</sup>             | 5.1 x 10 <sup>-5</sup>             | 4.9 x 10 <sup>-5</sup>             |
|                                    | 30 x 10 <sup>-2</sup>                             | 1.3 x 10 <sup>-1</sup>             | 1.8 x 10 <sup>-3</sup>             | 9.4 x 10 <sup>-5</sup>             | 7.8 x 10 <sup>-5</sup>             |
|                                    | 40 x 10 <sup>-2</sup>                             | 9.8 x 10 <sup>-2</sup>             | 1.4 x 10 <sup>-3</sup>             | 1.5 x 10 <sup>-4</sup>             | 5.9 x 10 <sup>-5</sup>             |

| pH                                   | [S <sub>2</sub> O <sub>8</sub> <sup>2-</sup> ] /M | k <sub>obs1</sub> /s <sup>-1</sup> | k <sub>obs2</sub> /s <sup>-1</sup> | k <sub>obs3</sub> /s <sup>-1</sup> | k <sub>obs4</sub> /s <sup>-1</sup> |
|--------------------------------------|---|------------------------------------|------------------------------------|------------------------------------|------------------------------------|
| <b>aprox. 0</b> <sup>(c)</sup>       | 2.5 x 10 <sup>-3</sup>                            | 0.8 x 10 <sup>-2</sup>             | 2.4 x 10 <sup>-3</sup>             |                                    |                                    |
| <b>(HClO<sub>4</sub> 1.0 M)</b>      | 5.0 x 10 <sup>-3</sup>                            | 1.8 x 10 <sup>-2</sup>             | 2.1 x 10 <sup>-3</sup>             | 0.7 x 10 <sup>-4</sup>             | 0.6 x 10 <sup>-4</sup>             |
| <b>I = 1.0 M (NaClO<sub>4</sub>)</b> | 7.5 x 10 <sup>-3</sup>                            |                                    | 3.7 x 10 <sup>-3</sup>             |                                    |                                    |
|                                      | 10 x 10 <sup>-3</sup>                             | 2.2 x 10 <sup>-2</sup>             | 3.4 x 10 <sup>-3</sup>             | 2.1 x 10 <sup>-4</sup>             | 1.5 x 10 <sup>-4</sup>             |
|                                      | 15 x 10 <sup>-3</sup>                             | 2.1 x 10 <sup>-2</sup>             | 4.0 x 10 <sup>-3</sup>             | 2.7 x 10 <sup>-4</sup>             | 2.4 x 10 <sup>-4</sup>             |
|                                      | 20 x 10 <sup>-3</sup>                             | 2.2 x 10 <sup>-2</sup>             | 4.9 x 10 <sup>-3</sup>             | 4.0 x 10 <sup>-4</sup>             | 3.8 x 10 <sup>-4</sup>             |
|                                      | 25 x 10 <sup>-3</sup>                             | 2.1 x 10 <sup>-2</sup>             | 5.0 x 10 <sup>-3</sup>             | 6.1 x 10 <sup>-4</sup>             | 5.7 x 10 <sup>-4</sup>             |
|                                      | 30 x 10 <sup>-3</sup>                             | 2.5 x 10 <sup>-2</sup>             |                                    |                                    |                                    |
| <b>aprox. 0.3</b> <sup>(c)</sup>     | 2.5 x 10 <sup>-3</sup>                            | 0.7 x 10 <sup>-2</sup>             | 1.2 x 10 <sup>-3</sup>             |                                    |                                    |
| <b>(HClO<sub>4</sub> 0.5 M)</b>      | 5.0 x 10 <sup>-3</sup>                            | 1.5 x 10 <sup>-2</sup>             | 2.1 x 10 <sup>-3</sup>             | 0.2 x 10 <sup>-4</sup>             | 0.1 x 10 <sup>-4</sup>             |
| <b>I = 1.0 M (NaClO<sub>4</sub>)</b> | 7.5 x 10 <sup>-3</sup>                            | 1.1 x 10 <sup>-2</sup>             | 2.1 x 10 <sup>-3</sup>             |                                    |                                    |
|                                      | 10 x 10 <sup>-3</sup>                             | 1.7 x 10 <sup>-2</sup>             | 2.4 x 10 <sup>-3</sup>             | 1.5 x 10 <sup>-4</sup>             | 9.7 x 10 <sup>-4</sup>             |
|                                      | 15 x 10 <sup>-3</sup>                             | 1.6 x 10 <sup>-2</sup>             | 2.5 x 10 <sup>-3</sup>             | 1.9 x 10 <sup>-4</sup>             | 1.7 x 10 <sup>-4</sup>             |
|                                      | 20 x 10 <sup>-3</sup>                             | 2.0 x 10 <sup>-2</sup>             | 3.5 x 10 <sup>-3</sup>             | 2.2 x 10 <sup>-4</sup>             | 2.1 x 10 <sup>-4</sup>             |
|                                      | 25 x 10 <sup>-3</sup>                             | 1.7 x 10 <sup>-2</sup>             | 3.6 x 10 <sup>-3</sup>             | 4.2 x 10 <sup>-4</sup>             | 2.22 x 10 <sup>-4</sup>            |
|                                      | 30 x 10 <sup>-3</sup>                             | 2.3 x 10 <sup>-2</sup>             |                                    |                                    |                                    |
| <b>aprox. 1</b> <sup>(c)</sup>       | 2.5 x 10 <sup>-3</sup>                            |                                    | 3.7 x 10 <sup>-3</sup>             |                                    |                                    |
| <b>(HClO<sub>4</sub> 0.1 M)</b>      | 5.0 x 10 <sup>-3</sup>                            |                                    | 4.3 x 10 <sup>-3</sup>             | 2.2 x 10 <sup>-4</sup>             | 2.0 x 10 <sup>-4</sup>             |
| <b>I = 1.0 M (NaClO<sub>4</sub>)</b> | 7.5 x 10 <sup>-3</sup>                            |                                    | 4.2 x 10 <sup>-3</sup>             | 3.9 x 10 <sup>-4</sup>             |                                    |
|                                      | 10 x 10 <sup>-3</sup>                             | 2.3 x 10 <sup>-2</sup>             | 4.1 x 10 <sup>-3</sup>             | 3.7 x 10 <sup>-4</sup>             |                                    |
|                                      | 15 x 10 <sup>-3</sup>                             | 2.6 x 10 <sup>-2</sup>             | 4.8 x 10 <sup>-3</sup>             | 6.3 x 10 <sup>-4</sup>             | 5.2 x 10 <sup>-4</sup>             |
|                                      | 20 x 10 <sup>-3</sup>                             | 3.0 x 10 <sup>-2</sup>             | 4.9 x 10 <sup>-3</sup>             | 6.9 x 10 <sup>-4</sup>             | 6.8 x 10 <sup>-4</sup>             |
|                                      | 25 x 10 <sup>-3</sup>                             | 3.0 x 10 <sup>-2</sup>             | 5.7 x 10 <sup>-3</sup>             | 9.7 x 10 <sup>-4</sup>             | 9.5 x 10 <sup>-4</sup>             |
|                                      | 30 x 10 <sup>-3</sup>                             | 3.2 x 10 <sup>-2</sup>             |                                    |                                    |                                    |

(a) [Na-Cube] = 28.8 μM

(b) [K-Cube] ≈ 239 μM

(c) [Na-Cube] = 17.7 μM

